Acousto-Optic Modulation with Etalon for Laser Scanning

Sophia TenHuisen
Mentor: Georg Raithel
Graduate Student Mentors: Jamie MacLennan and Lu Ma
University of Michigan Physics REU
August 11, 2017

Rydberg atoms are atoms with large principle quantum numbers, n, in highly excited states. Since many properties scale as powers of the principle quantum number, many properties are exaggerated in these systems. For example, atomic radius scales as n^2, while polarizability scales as n^7. Combined with their relatively long lifetimes, this makes them ideal candidates for studying such interactions. The Raithel group works with rubidium and cesium, both of which have only one valence electron, allowing them to be modeled very accurately with models similar to those for hydrogen. Furthermore, there are potential applications for these systems in quantum computing and communication.

Spectroscopy is the primary means for studying these atoms, which requires scanning the frequency of the laser across a range of frequencies. By measuring which frequencies are absorbed by an atomic sample, energies such as molecular binding energies and fine and hyperfine atomic structures can be made. For example, the grad student I worked with this summer, Jamie MacLennan, is working on an experiment to measure the binding energies of Rydberg molecules, which consist of an excited Rydberg atom and a ground state Rydberg atom, bound together in a scattering interaction. She aims to measure the binding energies in both isotopes of rubidium, Rb-85 and Rb-87, as well as that of different spin states and hyperfine structures. Currently she uses a Fabry-Perot interferometer to scan a 960nm laser, but this summer I worked on developing an alternative method, using an acousto-optic angle modulation combined with an etalon. The Fabry-Perot currently used has a complicated calibration process, and suffers a large thermal drift, limiting experiments to short scans. The new device, however, offers a simpler calibration process, due to the linear relationship between key variables, allowing for more precise laser tuning. In addition, it has the potential to have lower long-term and thermal drift. Pictures of the device are shown on the last page.

An acousto-optic modulator (AOM) is based on very similar principles to Bragg diffraction. A radio frequency (rf) wave passes through a crystal, creating pressure waves which alter the index of refraction of the crystal, causing it to behave as a diffraction grating. By carefully positioning the angle at which light enters the crystal, the AOM can be optimized to divert the majority of the power of the incoming beam into the first diffraction order. As the rf frequency to the device is changed, the separation between the two diffraction orders changes, according to the relationship $\theta_{sep} = \frac{\lambda_{light}\, f}{v_{sound}}$, where f is the rf

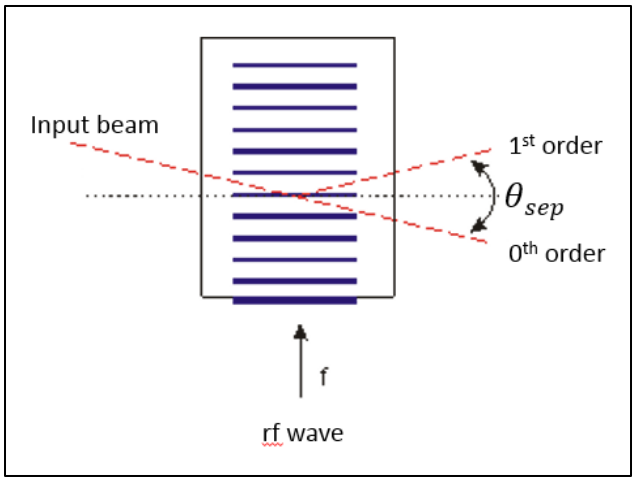

Figure 1: Schematic of an acousto-optic modulator

frequency input to the crystal. Since the position of the zeroth order is unaffected by the rf frequency, this amounts to adjusting the position of the first order output (fig. 1).

In our system, light is fed into an AOM, and the output light from the AOM is then passed into an etalon. An etalon consists of a cavity with two highly reflective surfaces facing one another, such that light will reflect back and forth between the two surfaces many times before emerging from the etalon. The phase of the emerging light depends on the number of times it has been reflected, and thus waves which have been reflected different numbers of times will form an interference pattern. This phase difference between waves is given by $\delta = \frac{2\pi\, v_{light}}{c}\ 2\, n\, d \cos\varphi$, where n is the index of refraction of the etalon (in our case 1.4509), d is the thickness of the etalon (6.743 mm in our case), and φ is the angle the light travels at, relative to the normal to the etalon surfaces (fig. 2).

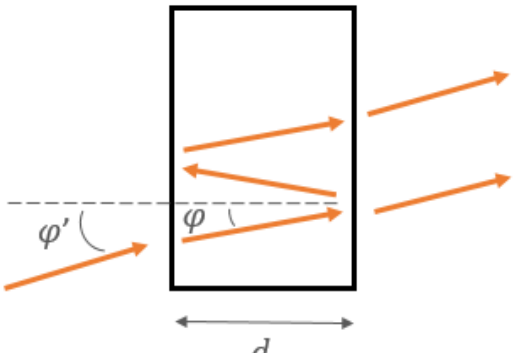

Figure 2: path of light through etalon

To modulate the laser frequency, we monitor the power output of the first order beam with a photodiode. This photodiode is connected to a control circuit, and locked to an intermediate power value. This allows us to fix the phase difference between waves, and thus, when the rf frequency is changed, the control circuit sends a signal to the laser to adjust its current output, altering the frequency of light emitted, such that the power on the photodiode remains constant as the rf frequency (and therefore angle of incidence of light on the etalon) is varied. Working from the equation previously given for the phase difference, δ, and using the small angle approximation, it can be shown that the rate at which the frequency of light will be shifted in terms of the change in the angle of the AOM first order output is $\frac{dv_{light}}{d\varphi} \cong v_0 \frac{\varphi'}{n^2}$, which is approximately 45 GHz/degree for our design. Combining this with the formula for the change in angle in terms of the change in rf frequency for the AOM, this amounts to a shift in light frequency of 840 MHz for every MHz the rf frequency is changed. A Schematic is shown below (fig. 3).

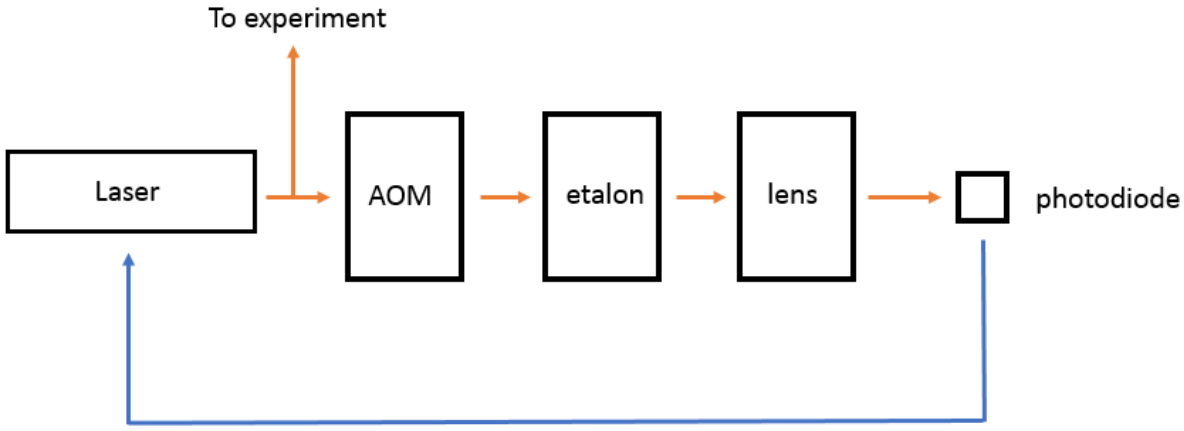

Figure 3: Schematic of laser lock circuit. Orange arrows denote a light beam, while the blue beam represents electronic feedback to the laser

A lens was used between the etalon to focus the first order and zeroth order beams to different spots. This also reduces the 'walk off' of the first order, or the change in the spatial location of the beam as the rf frequency is changed. Thus the lens allows us to monitor the first order without having to block off the zeroth order before the etalon, and without requiring a large photodiode. I chose a 2.5 focal length lens, to allow for sufficient separation between the zeroth and first orders, while minimizing the size of the device. The lens is held in a lens tube, which is held in the same mount as the etalon (fig. 5).

One of the important considerations for this device was temperature stability. Changes in temperature cause thermal expansion or contraction, which alter the length of the etalon, altering the interference pattern. As we lock the laser to a particular power output, it is important that any changes in the interference pattern are caused solely by changes in the rf frequency, and not by changes in the length of the etalon. The location of transmission peaks for the etalon shift to lower frequencies at a rate of 1993 MHz/°C, so we aimed to keep temperature fluctuations of the etalon smaller than 5 mK. This corresponds to a change in the peak transmission frequency of 9.97 MHz. To achieve this, the etalon and lens were mounted in a copper block, which rested on a Peltier thermos-electric cooler (TEC), which in turn rested on an aluminum heat sink (fig. 5). A small amount of thermal paste was used between the TEC and the heat skink and copper mount. The copper mount was then enclosed in a 3D printed box, with a filling fraction of 15% to insulate it from its surroundings (fig. 5). Although we were unconcerned about the temperature of the AOM, it too was mounted on an aluminum heat sink, because the temperature of the device depends strongly on the rf frequency passing through it (fig. 4). Thus to minimize the effect these variations had on the etalon, the AOM was also mounted on a heat sink. I made all heat sinks and mounts for components in the student shop. I designed the insulating box in Solidworks, and had it printed in the IT office in Randall.

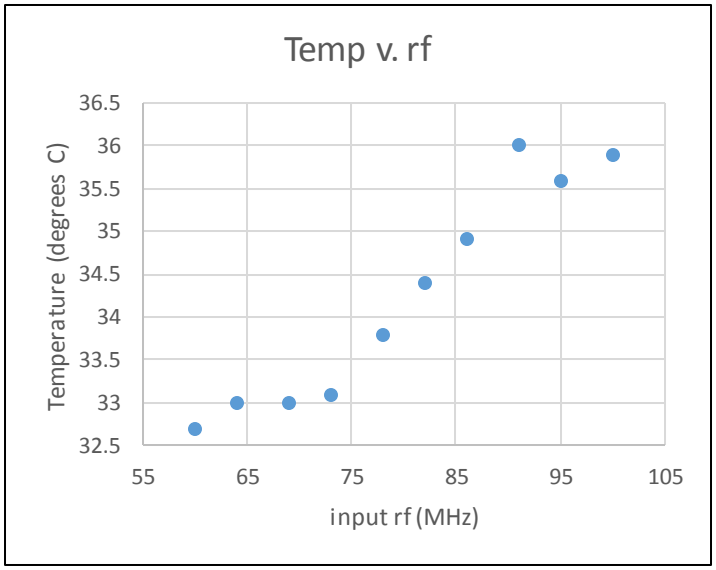

Figure 4: variation in AOM temperature as function of rf frequency

The final step in this project will be to optimize the position of the photodiode. The photodiode will be mounted between two aluminum disks, in the same lens tube as the achromatic lens. One disk has a slot through its diameter, while the other has a slot just to the side of its diameter, so that the two can be positioned relative to one another at any angle, determining the position for the photodiode. By tightening these disks between two mounting rings in the lens tube, the photodiode can be held in place. If the group decided to use this device in more widespread applications, a fiber-coupler should be added to the input of the AOM so that the device does not need to be realigned every time it is used. Lastly, the long-term and temperature stability of the device remain to be measured.

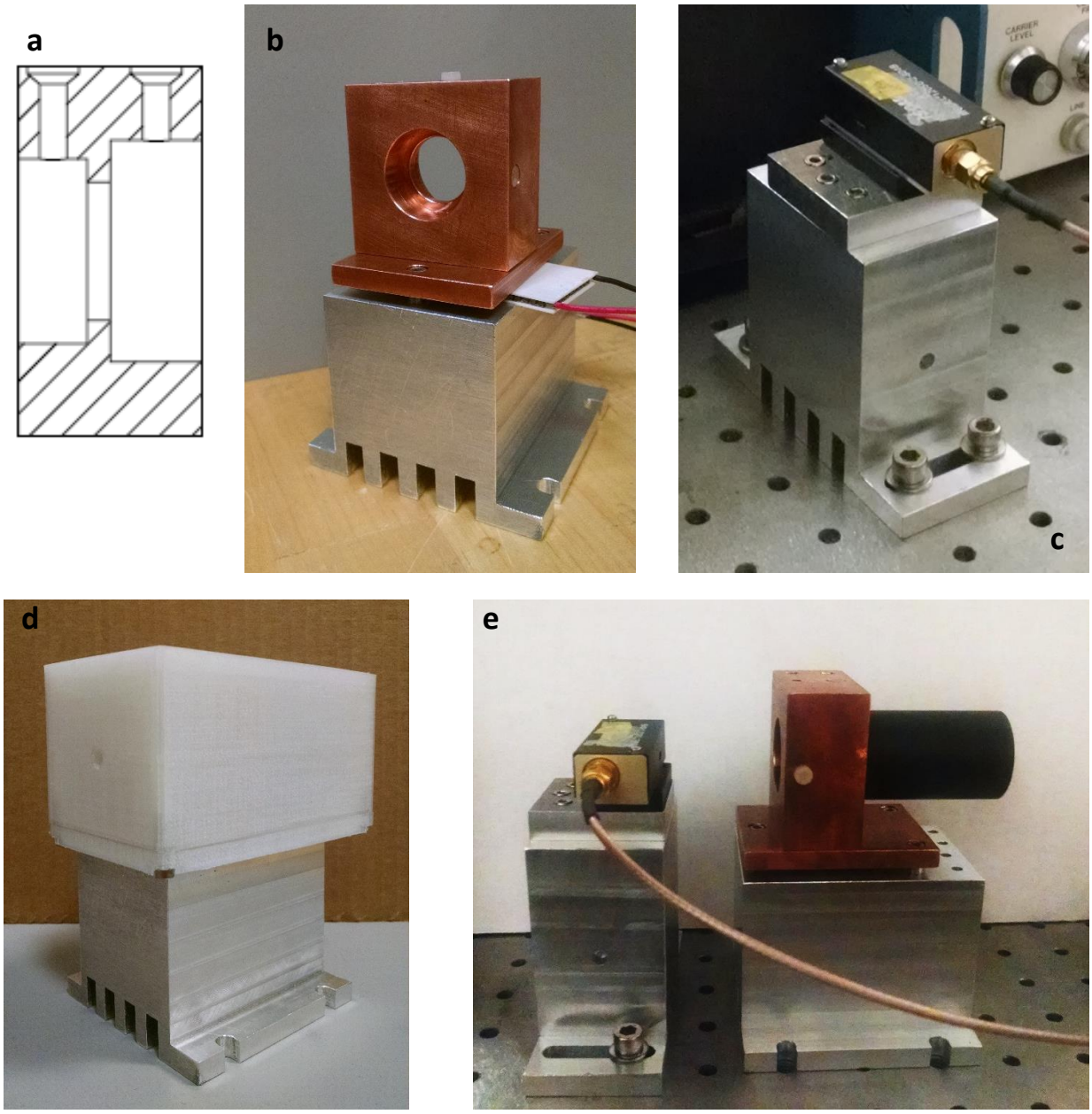

Figure 5: Images of the components machined for this device. (a) a cut showing the side view of the copper mount for the etalon and lens. The lens tube fits in the larger diameter hole, while the etalon drops in the other side. Both are held in place by set screws. (b) the copper mount for holding the etalon and achromatic lens, atop an aluminum heat sink, with the Peltier TEC nested between the two. (c) the AOM mounted atop an aluminum heat sink. (d) the etalon mount, enclosed in the 3D printed insulating box. (e) the system mounted on an optical table, with the plastic cover removed.

Thank you to my lab group for all their help and everything they've taught me. Thank you also to Jim Tice in the machine shop for all his help and his good humor. Lastly, thank you also to Myron Campbell, Jim Liu, and Angela Germaine for all their work organizing this program and making sure we got the most out of our time here. I'm very grateful to have had this opportunity.